International Journal of Nanomedicine

Dovepress
open access to scientific and medical research

Open Access Full Text Article

ORIGINAL RESEARCH

Development and in vitro evaluation of (β-cyclodextrin-g-methacrylic acid)/Na^+-montmorillonite nanocomposite hydrogels for controlled delivery of lovastatin

This article was published in the following Dove Press journal:
International Journal of Nanomedicine

Asif Mahmood[1,2]
Amara Sharif[2]
Faqir Muhammad[2]
Rai Muhammad Sarfraz[3]
Muhammad Asad Abrar[4]
Muhammad Naeem Qaisar[3]
Naveed Anwer[5]
Muhammad Wahab Amjad[6]
Muhammad Zaman[1]

[1]Department of Pharmaceutics, Faculty of Pharmacy, The University of Lahore, Lahore, Pakistan; [2]Institute of Pharmacy, Physiology and Pharmacology, University of Agriculture Faisalabad, Faisalabad, Pakistan; [3]Department of Pharmaceutics, College of Pharmacy, University of Sargodha, Sargodha, Pakistan; [4]Department of Pharmacy, Bahauddin Zakariya University, Multan, Pakistan; [5]Saulat Institute of Pharmaceutical Sciences, Quaid-I-Azam University, Islamabad, Pakistan; [6]Faculty of Pharmacy, Northern Border University, Arar, Saudia Arabia

Background: Hyperlipidemia is the elevation of low density lipoprotein levels resulting in fat deposites in arteries and their hardening and blockage. It is the leading cause of several life threatening pathological conditions like hypertension, cardiovascular diseases, diabetes etc.

Purpose: The objective of this study was to prepare and optimize nontoxic, biocompatible β-CD-g-MAA/Na^+-MMT nanocomposite hydrogels with varying content of polymer, monomer and montmorillonite. Moreover, lipid lowering potentials were determined and compared with other approaches.

Methods: β-CD-g-MAA/Na^+-MMT nanocomposite hydrogels (BM-1 to BM9) were prepared through free radical polymerization by using β-CD as polymer, MAA as monomer, MBA as crosslinker and montmorillonite as clay. Developed networks were evaluated for FTIR, DSC, TGA, PXRD, SEM, sol-gel fraction (%), swelling studies, antihyperlipidemic studies and toxicity studies.

Results: Optimum swelling (94.24%) and release (93.16%) were obtained at higher pH values. Based on R^2 and *"n"* value LVT release followed zero order kinetics with Super Case II transport release mechanism, respectively. Tensile strength and elongation at break were found to be 0.0283MPa and 94.68%, respectively. Gel fraction was between 80.55 – 98.16%. Antihyperlipidemic studies revealed that LDL levels were markedly reduced from 522.24 ± 21.88mg/dl to 147.63 ± 31.5mg/dl. Toxicity studies assured the safety of developed network.

Conclusion: A novel pH responsive crosslinked network containing β-CD – g – poly (methacrylic acid) polymer and MMT was developed and optimized with excellent mechanical, swelling and release properties and lipid lowering potentials.

Keywords: lovastatin, nanocomposite networks, montmorillonite, antihyperlipidemic and toxicity

Correspondence: Asif Mahmood
Faculty of Pharmacy, University of Lahore, 1-KM Defence Road, Bhobatian Chowk, Raiwind Road, Lahore, Pakistan
Tel +92 345 105 2514
Email asif.mahmood@pharm.uol.edu.pk

Faqir Muhammad
Institute of Pharmacy, Physiology and Pharmacology, University of Agriculture Faisalabad, Faisalabad, Pakistan
Tel +92 305 971 2950
Email faqir@uaf.edu.pk

Introduction

Hydrogels are three-dimensional polymeric networks with the capability to absorb large amounts of water and other biological media in their crosslinked framework. These undergo volume transitions in response to different stimuli, ie, temperature, pH, and solvent composition etc. Due to their elastic and rubbery nature, these are employed in tissue engineering, the pharmaceutical sector as drug delivery devices, agriculture, sensors, and as precursor for a number of organs, artificial skin, and heart linings etc. But they have certain limitations like poor physical and mechanical properties.[1,2]

submit your manuscript | www.dovepress.com
DovePress
http://doi.org/10.2147/IJN.S209662

Nanostructures like montmorillonite (MMT), laponite, silicates, and attapulgite etc, have already been incorporated into various types of networks to improve their mechanical strength.[3] MMT is a silicate with low cost, hydrophilic nature, greater surface area and biocompatibility. It presents excellent swelling in aqueous media and has exceptional cation exchange ability. Silanol groups (-Si – OH) on the surface participate in hydrogen bonding to produce a network with excellent mechanical properties to prolong drug release.[4–6]

Lovastatin (LVT), a BCS class II drug, is a cholesterol-lowering agent which is widely prescribed in hyperlipidemia. LVT (half life, 1 – 2 hours) is activated within the body due to break-down of its lactone part into hydroxyl acid by cytochrome P450 3A4 that inhibits HMG Co – A reductase, responsible for cholesterol biosynthesis. It has poor oral bioavailability (<5%) due to rapid metabolism in liver and intestine. Sustained delivery is a feasible approach to minimize the effects of individual variation and to avoid quick clearance of LVT.[7–10]

β-cyclodextrin (β-CD) is a hollow truncated cone-shaped cyclic compound. Hydroxyl (-OH) groups on the outer surface are involved in a variety of chemical reactions involving reduction, ester formation and polymerization etc. It is widely used in solubility enhancement and for other applications due to its low cost and non-toxic nature. Networks with β-CD as polymer in their composition offer adsorption ability for most drugs.[11–13]

Nanocomposite networks have good mechanical strength due to non-covalent interactions among polymeric materials and inorganic nanostructures. Different techniques, ie, in situ template synthesis, solution intercalation, in situ intercalative polymerization, and melt intercalation etc, are used. Polymerization involving intercalation of the nanomaterials is widely used and accepted. Therapeutic potentials of paclitaxel-, ofloxacin-, and paracetamol- etc loaded hydrogel nanocomposites have already been proven in the literature.[14–17]

In the present work, successful efforts have been made with an objective to prepare high-strength, non-toxic, and biocompatible β-CD-g-methacrylicacid (MAA)/MMT-based nanocomposite networks through graft polymerization for controlled delivery of LVT. To evaluate effects of MMT clay, MAA, methylene bisacrylamide (MBA) contents on degree of swelling and release of LVT. Lipid-lowering potential of LVT-loaded NC hydrogels was determined.

Materials and methods

Materials

LVT (99% pure) was purchased from and supplied by Beijing Mesochem Technology Co., Ltd, China. β-CD (99%), methacrylic acid (99%), ammonium persulfate (99%), N, N-methylene bisacrylamide (99%), and methanol (99.7%) were purchased from Sigma-Aldrich Co., St Louis, MO, USA. Potassium dihydrogen phosphate, orthophosphoric acid, and sodium hydroxide were purchased from Dae-Jung, Korea. Distilled water was freshly prepared in the research lab of the Faculty of Pharmacy, The University of Lahore. All the chemicals used were of analytical grade.

Methods

Synthesis of pH-responsive β-CD-co-poly (methacrylic acid) nanocomposite networks

Free radical polymerization is a widely employed technique for synthesis of polymeric networks. In the current work, a slightly modified aqueous free radical polymerization technique was utilized to prepare nanocomposite networks. In the first step, a specific amount of MMT was dispersed into deionized water and subjected to stirring for 2 hours followed by its sonication for 1 hour. MMT suspension was than filtered, purified, and remaining mass was separated and dried for further use. An accurate quantity of β-CD was mixed in deionized water on a hot plate magnetic stirrer (Velp Scientifica, Italy) with continuous stirring and gentle heating until the formation of a transparent solution. Ammonium persulfate (APS) and MBA were dissolved separately in a small volume of deionized water. A defined amount of MAA was added into APS solution with uniform stirring and slight heating until a clear solution was obtained. MAA solution was added into β-CD solution drop-wise using a disposable syringe. Finally, MBA solution was transferred into the resultant mixture to initiate crosslinking process. The whole reaction mixture was weighed and distilled water was used for final volume makeup. Pre-treated MMT was added into this mixture and stirred for 40 minutes in order to ensure uniform distribution. The resultant mixture was transferred into glass test tubes. These tubes were purged with nitrogen gas, vortexed, and sonicated to remove any dissolved oxygen. After that, their open ends were sealed with aluminum foil and shifted to digital water bath. The temperature was increased in a stepwise fashion, ie, 45°C for 1 hour, 50°C for 2 hours, 55°C for 3 hours, 60°C for 6 hours, and at 65°C for 12 hours in order to avoid bubble

Table 1 Composition of developed hydrogel nanocomposites

Formulation	β-cyclodextrin (g)	Methacrylicacid (g)	Methylenebisacrylamide (g)	Ammonium persulfate (g)	Montmorillonite (g)
BM-1	2	15	1.5	0.75	0
BM-2	2	20	1.5	0.75	0
BM-3	2	30	1.5	0.75	0
BM-4	2	20	2.0	0.75	0
BM-5	2	20	2.2	0.75	0
BM-6	2	20	2.4	0.75	0
BM-7	2	20	1.5	0.75	2.2
BM-8	2	20	1.5	0.75	4.4
BM-9	2	20	1.5	0.75	6.6

formation in the molds. After polymerization, NC hydrogel rods were removed and cut into discs using a sharp-edged blade. NC hydrogel discs were soaked in water and ethanol mixture (50:50) to remove leftover unreacted species. Washing was continued until a constant pH value of washing media was attained. Finally, discs were vacuum oven dried at 40°C to constant weight.[18] Different formulations were prepared by varying the ratios of ingredients, as shown in Table 1.

Drug loading

Diffusion assisted swelling method was adapted for loading of LVT into the developed NC networks. LVT was utilized for loading purposes. LVT 1% solution was prepared by dissolving LVT in phosphate buffer (pH 7.4) containing 250 mg sodium lauryl sulfate (SLS) with final volume 100 mL. SLS was added to promote dissolution of LVT.[19] The pH of drug solution was maintained basic due to pH sensitivity of NC networks. Preweighed hydrogel discs were soaked in 1% LVT solution for 48 hours or the time up to which optimal swelling was achieved. Swollen NC hydrogel discs were removed from LVT solution and rinsed with distilled water to flush the surface LVT. LVT-loaded networks were dried in hot air oven (Memmert, Japan) at 40°C until constant weight was achieved.[20]

Sol – Gel fraction studies

For determination of reactants exhausted while developing nanocomposite networks, Sol – Gel fraction (%) of NC networks was determined. Sol contents are the dissolved non-reactive ingredients of polymerization reaction. A known quantity of NC networks was taken and crushed into 2 mm size pieces with a pestle and mortar. Extraction was carried out in Soxhlet apparatus at 95±5°C using boiling water for 4 hours. Soluble reactants were condensed back in boiling water in a round-bottom flask. After that, networks were removed and dried at room temperature followed by vacuum oven drying at 40°C–45°C.[21]

Gel fraction was calculated by using the following formulas:

$$Sol\ fraction = \frac{M_i - M_a}{M_a}$$

$$Gel\ fraction = 100 - sol\ fraction$$

where, Mi is the initial mass of NC hydrogels and Ma is the final mass of NC hydrogels after the completion of experiment.

Chemical analysis by Fourier-transform infrared spectroscopy (FTIR)

FTIR spectra of pure β-CD, LVT, blank NC networks, and LVT-loaded NC networks were recorded using FTIR spectroscopy (Bruker Tensor 27, Germany). Fabricated networks, both blank and LVT-loaded NC networks, were crushed powdered using and dried at 45°C before scanning them at a range of 400–3,500 $cm.^{-1}$ IR spectroscopy basically works on the principle that chemical bonds within individual components and developed network absorb IR radiations and give respective peaks.[22]

Thermal analysis

Thermal analysis of pure LVT, β-CD, blank formulation, and LVT-loaded NC networks was performed by thermogravimetric analyzer (West Sussex, UK). Changes in heat of fusion and stability of ingredients with the increase of temperature were recorded and presented as differential scanning calorimetry (DSC) and thermal gravimetric analysis (TGA) thermograms, respectively. Practically, a sample (0.5–5 mg) was placed on a platinum pan with attached microbalance. The sample was heated under

nitrogen gas environment from 0°C–600°C at a heat rate of 20°C/min and thermograms were recorded.[23]

Powdered X-ray diffraction studies (PXRD)

PXRD analysis of pure ingredients, blank, and LVT-loaded NC networks was performed to determine their nature, ie, crystalline or amorphous. Briefly, powdered mass of each sample was loaded onto plastic sample holders and these were covered with smooth glass slide. X-ray diffractometer (X ray analytical Xpert powder diffractometer) was operated and peaks in the form of diffractograms were recorded at a scanning range of 10–100° with an angle of 2θ at a rate of 3°per min. Copper k_α was used as radiation source with wavelength 1.542 Å.[24]

Morphological analysis by scanning electron microscopy (SEM)

NC networks were soaked in phosphate buffer (pH 7.4) at room temperature until complete swelling occurred. Swollen networks were freeze dried overnight at −55°C in lyophilizer (Christ Alpha 1–4 LD, Japan) to remove solvent. Samples were prepared by crushing the lyophilized NC networks thereby exposing their internal structure. Surface morphology was recorded by using SEM. JEOL Analytical Scanning Electron Microscope (JSM-6490A, JEOL, Tokyo, Japan) was operated at different magnification powers and photomicrographs were captured.[24]

Mechanical properties

Developed NC networks had a cylindrical shape of 5 mm diameter and 45 mm length in glass molds before performing the uniaxial tensile strength measurements. Tensile tester equipped with 10 kN load chamber and TIRA software was operated as per American Society of Testing Materials guidelines. Briefly, a sample with smooth surfaces was dimensioned by using a specimen cutter. The sample was mounted between static and mobile jaws of the tester. The instrument was operated at 50 mm/min crosshead rate in ambient conditions. Stress (σ) ie, forces per unit area and strain (ε) ie, change in length as compared to initial or actual length were calculated by using the formulas:[25]

$$\sigma = \frac{F}{\pi r^2}$$

where, F = actual load exerted on the NC hydrogel sample, r = radius of the sample.

$$\varepsilon = \frac{l - lo}{lo}$$

Where, l = final length and lo = original length.

Swelling studies

Swelling behavior of developed NC networks was observed by performing swelling experiments at pH 1.2 and pH 7.4. Dried NC hydrogel discs from each formulation were chosen and soaked in 100 mL of respective buffer media of stated pH value. Samples were removed at pre-defined time intervals, ie, 0.5, 1, 1.5, 2, 3, 4, 6, 8, 10, 12, 14, 18, and 24 hours. Surface of discs was blotted with filter paper to absorb excess swelling media.[23] Studies were continued until equilibrium swelling was not achieved. Swelling ratio (q) was calculated by using the following expression:

$$q = \frac{Ws}{Wd}$$

where, Ws is the weight of swollen NC networks and Wd is the weight of dried NC networks.

Dissolution properties

United States Food and Drug Administration (FDA), Centre for Drug Evaluation and Research recommended dissolution conditions for LVT were used. LVT release studies were performed on USP-type II apparatus (PTCF II Pharma Test, Germany) at 100 rpm. Aliquots of 5 mL were removed at specified time intervals on the basis of swelling experiments. Each 5 mL sample removal compensated for by equal volume of fresh dissolution media, ie, pH 1.2 or pH 7.4 into the same vessel to maintain sink conditions. Samples were filtered and diluted followed by LVT estimation at 238 nm using UV-visible spectrophotometer (UV – 1600, Shimadzu, Germany). Temperature during the entire analysis was maintained at 37±0.5°C.[20]

Drug release data analysis

To determine the pattern of LVT release from NC networks and best fit kinetic model, release data of all formulations were processed through DD solver adds in Microsoft Excel program by applying kinetic models, ie, first order model, Higuchi model, zero order and Korsemeyer Peppas model.[20] Release data (%) with respect to defined time intervals (hours) were loaded onto software by selecting specific kinetic model from dissolution data modeling. Results of each kinetic model include rate constant, R^2 value, time required for 25%, 50%, 75%, 80%, and 90% drug release, and provide prediction of particular release kinetics. Best fit model and mechanism of release were determined from the results of R^2 and value of n, respectively. Value of "n" equal to 0.45 governed Fickian diffusion, values between 0.45–0.89 proved non-fickian diffusion or anomalous diffusion while value of "n" equal to 0.89 highlighted typical zero order or Case – II transport.

Zero order kinetics

$$Qt = Qo - Kot$$

First order kinetics

$$LnQt = LnQ_o - K_1 t$$

Higuchi kinetic model

$$Q_t = K_h t^{1/2}$$

Where, Qo = total amount of LVT in NC networks, Q_t = amount of LVT release at time't' and K_o, K1 and Kh are the rate constants of the respective executed kinetic model.

To determine mode of drug release, release data were also processed through Korsemeyer Peppas model:

$$\frac{Mt}{M\infty} = Kt^n$$

Where M_t/M_∞ is portion of LVT released at time t, K is drug release rate constant and "n" is release exponent.

Statistical analysis of data

Swelling studies, release data, and antihyperlipidemic potentials of different formulations were statistically evaluated by applying ANOVA by using GraphPad Prism version 7.1.

In vivo evaluation

Antihyperlipidemic and toxicity studies were reviewed and approved by Institutional Research Ethics Committee (IREC) of The University of Lahore vide approval number IREC-2018–57. IREC guidelines were followed for the welfare of experimental animals (notification number IREC-2018–57). IREC guidelines, for executing experiments on animals follow protocols of US FDA that are furnished under International Conference on Harmonisation guidelines.

Antihyperlipidemic activity

Animals and experimental procedures

Healthy albino rabbits (n=18, 1.3–1.6 kg) were taken from the animal house of Faculty of Pharmacy, University of Lahore. These were grouped into three groups, ie, Group A (hyperlipidemic control), Group B (treated with LVT suspensions), and Group C (treated with LVT-loaded NC networks). Animals were kept in stainless cages at 20°C −30°C temperature in 12 hour light/dark cycle with free access to food and water for 10 days to acclimatize to the laboratory conditions. In group A, B, and C, hyperlipidemia was induced by providing an atherogenic diet for 4 weeks. Atherogenic diet was prepared by mixing cholesterol (500 mg/kg) in 10 mL mixture of coconut oil and egg yolk. All the experimental animals were fasted for 14 hours. Blood samples were collected from jugular vein using insulin syringe to check hyperlipidemic profile. After that, LVT suspensions (Group B) and crushed LVT-loaded NC networks (Group C) were administered orally (6 mg/kg/day) for 30 days. Blood samples (2−3 mL) were collected on 30th day of treatment in EDTA tubes. Total cholesterol, high density lipoprotein (HDL), low density lipoprotein (LDL), and triglyceride (TG) levels were biochemically determined by Alkhidmat Laboratories, Faisalabad, Punjab, Pakistan.

Acute oral toxicity studies

Impact of developed carrier system on physical activity and major organs of albino rabbits (1.5–2 kg) was observed through physical parameters and microscopic examination. OECD guidelines for testing chemicals were strictly followed. Animals were kept in dark/light cycle (12 hours) for 1 week to acclimatize to the conditions. They were housed in stainless steel cages with free access to tap water and standard diet. Before the day of the experiment, animals were fasted for 12 hours with free access to water. Animals (n=6) were grouped into two groups (n=3), ie, Group A and Group B. Group A was kept as control and Group B was administered crushed carrier system (5 g/kg) with the aid of water. The study was continued for 14 days. During this period, intense observation of each group was performed in respect of body weight, water and food intake, skin allergies, hematology, ALT, and AST levels, lipid and renal profile, and other physical variabilities. At the end of the 14th day, animals were re-weighed, scarified, and vital organs, ie, heart, kidney, lungs, liver, stomach, spleen, and intestine were removed, washed, and stored in a formalin solution (10%) in separate containers.

Results and discussion

Sol – Gel fraction

All the formulations had a gel fraction of 80.55%–98.16%. Optimum gel fraction with increasing contents of MMT, MAA, and MBA was 95.22%, 80.18%, and 91.85%, respectively. Successive rise in gel fraction was seen with the increase increment of clay, monomer, and cross-linker. Consequences of MMT, MAA, and MBA on gel fraction in developed formulations (BM-1 to BM-9) are reported in Figure 1.

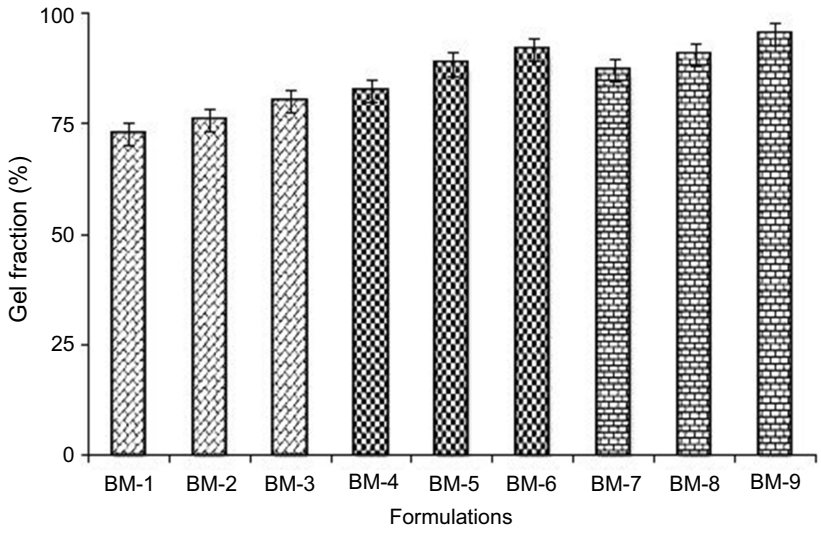

Figure 1 Effect of increasing contents of polymer, monomer, and crosslinker on gel fraction.

Structural analysis

FTIR spectra of pure β-CD, MAA, LVT, physical mixture, blank NC networks, and loaded NC networks reinforced with different increments of MMT were recorded and their interpretation was done. No distinct changes were observed when these were individually scanned, while spectrum of developed networks clearly exhibited LVT peak shifting. All the FTIR results are shown in Figure 2.

Thermal analysis

DSC thermograms of neat ingredients and fabricated networks were recorded. Stability of developed NC hydrogels was markedly increased even at elevated temperatures. DSC thermograms of pure LVT, β-CD, MAA, MMT, and LVT-loaded NC networks are presented in Figure 3.

TGA curves of individual ingredients as well as fabricated NC networks were recorded to estimate %weight loss with sequential rise of temperature. TGA studies proved that more than 48% mass remained intact even at temperature higher than 374°C. All the TGA thermograms are presented in Figure 4.

X-ray diffraction (XRD) studies

XRD patterns of individual ingredients as well as grafted network were recorded to check their nature, ie, crystalline or amorphous. Each diffractogram exhibited a unique pattern and peak intensity. Pure LVT exhibited sharp and intense peaks due to its crystalline nature, while in the case of grafted NC network its crystalline nature was modified into amorphous nature. XRD diffractograms are presented in Figure 5.

SEM

SEM photomicrographs of developed β-CD-co-poly (MAA) NC networks were captured at different magnification powers to observe surface morphology of newly developed NC hydrogels as shown in Figure 6. Surface morphology revealed porous surfaces of test samples.

Mechanical properties of nanocomposite networks

Tensile strength and optimum elongation break were determined. Results are summarized in Figure 7. Different results in respect of stress and strain were obtained against increasing proportions of MMT clay. Tensile strength was potentiated from 0.010–0.0283 MPa and optimum elongation break was increased from 50.39%–94.68%.

Effect of MMT, MAA, and MBA on LVT loading and swelling of NC networks

Effect of variable quantities of MMT, MAA, and MBA on LVT loading and swelling of the newly developed network were observed, as shown in Figure 8. Q value was calculated by dividing initial mass of NC networks by final mass at a pre-defined time interval. During the entire swelling period formulations retained their shape without any sort of breakage. Overall swelling of the NC hydrogels was promoted with the rise of MAA content, while decline

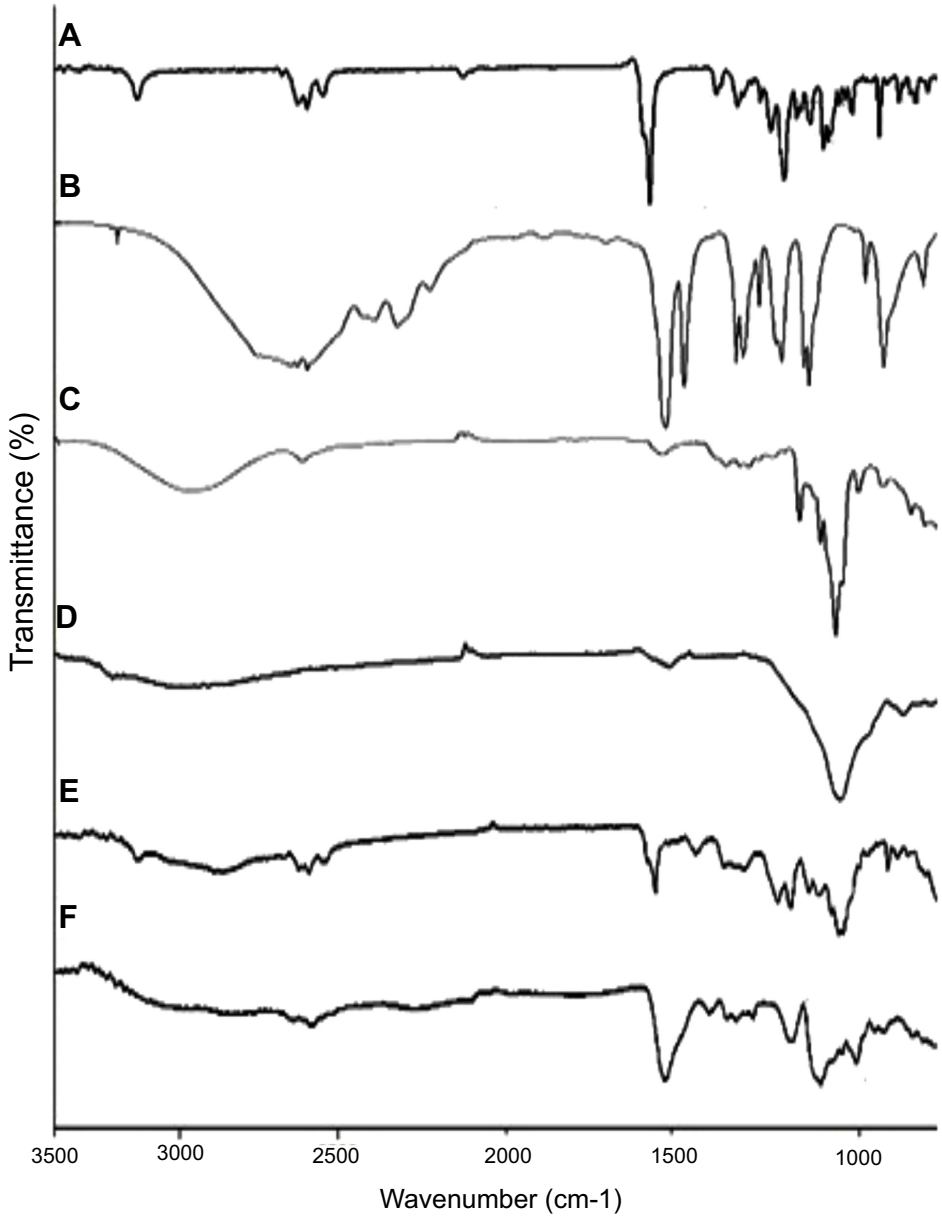

Figure 2 FTIR spectra of LVT (**A**), methacrylic acid (**B**), β-cyclodextrin (**C**), MMT (**D**), physical mixture (**E**) and LVT-loaded NC networks (BM-8) (**F**).
Abbreviations: FTIR, Fourier-transforminfrared spectroscopy; MMT, montmorillonite; LVT, lovastatin; NC, nanocomposite.

in swelling was seen with the rise of MBA and MMA contents. Variable amount of LVT was loaded into the prepared NC hydrogel discs depending upon quantity, characteristic features of the ingredients, and pH of the medium, as reflected in Figure 8 (G, H).

LVT release studies and release data modeling

LVT release profile was determined in β-CD-g-poly (MAA) NC networks at two pH values ie, 1.2 and 7.4. Results are summarized in Figure 9. At pH 1.2, LVT release was ranging between 6.05%–10.85%. At this condition, optimum release, ie, 10.85%, was delivered by formulation BM-4. While at pH 7.4, LVT release was ranging between 71.44%–93.16% ($p<0.0001$), which is much higher than release at pH 1.2.

Release data were processed by applying kinetic models to find the best fit model and mechanism of release. All the developed formulations followed zero order kinetics with Super Case II transport as release mechanism. Results of kinetic models are shown in Table 2.

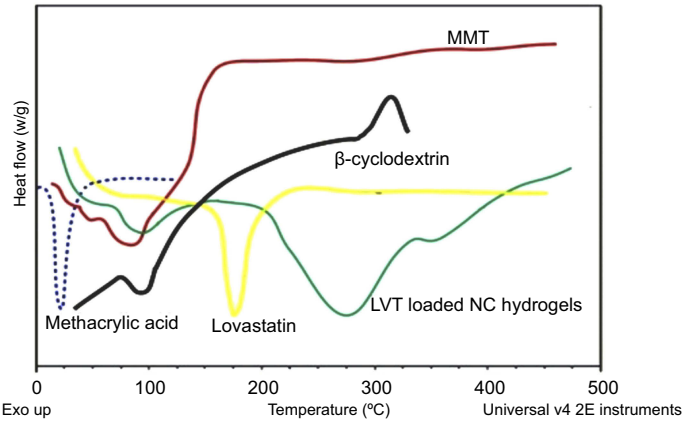

Figure 3 DSC thermograms.
Abbreviations: DSC, differentialscanning calorimetry; MMT, montmorillonite; LVT, lovastatin; NC, nanocomposite.

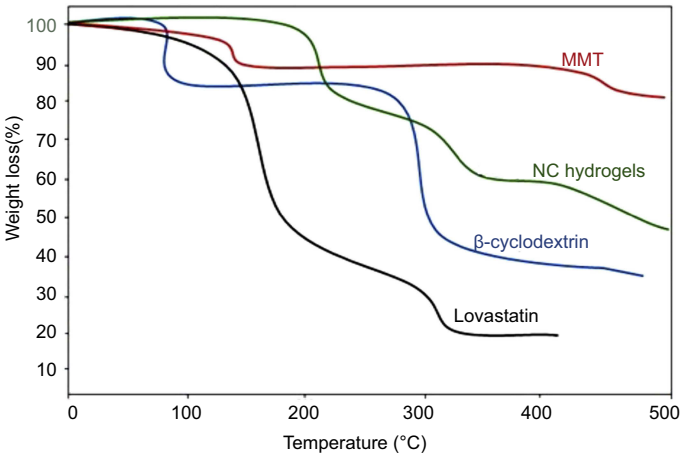

Figure 4 TGA thermograms.
Abbreviations: TGA, thermalgravimetric analysis; MMT, montmorillonite; NC, nanocomposite.

Antihyperlipidemic activity of LVT suspension and LVT-loaded NC networks

Hyperlipidemia was induced by administration of an atherogenic diet for 30 days. Total cholesterol, TG, LDL, and HDL were increased from 45.01±13.75 mg/dL to 945.11 ±616.91 mg/dL, 48.25±15.05 mg/dL to 77.53±6.45 mg/dL, 18.23±15.33 mg/dL to 522.24±21.88 mg/dL, and 24.55 ±5.31 mg/dL to 58.95±5.67 mg/dL, respectively. After the treatment period of 4 weeks of LVT suspension, total cholesterol, TG, and LDL levels were reduced from 945.11 ±616.91 mg/dL to 761±36.85 mg/dL, 77.53±6.45 mg/dL to 62±5.28 mg/dL, and 522.24±21.88 mg/dL to 390.11±28.1 mg/dL, respectively. HDL level was slightly increased from 58.95 ±5.67 mg/dL to 61.25±5.37 mg/dL. In contrast to this, significant reduction in total cholesterol (945.11±616.91 mg/dL to 277.23±12.1 mg/dL), TG (77.53±6.45 mg/dL to 38.86 ±2.66 mg/dL), and LDL (522.24±21.88 mg/dL to 147.63 ±31.5 mg/dL) was observed. HDL levels were increased from 58.95±5.67 mg/dL to 67.11±5.11 mg/dL. All the results are computed in Table 3.

Obtained results of different blood contents were statistically analyzed by using GraphPad Prism Version 7.0. ANOVA followed by Tukey's Multiple Comparison Test was employed. Parameters, including total cholesterol, TG, LDL, and HDL showed significant difference ($p<0.05$) when hyperlipidemic control was compared with LVT suspension and LVT-loaded NC network (Table 4). The only exception was comparative analysis of hyperlipidemic control vs LVT suspension for only a single parameter, eg, HDL, where results were non-significant. All the studied parameters confirmed that outcomes of LVT-loaded NC network compared to that of LVT suspension were

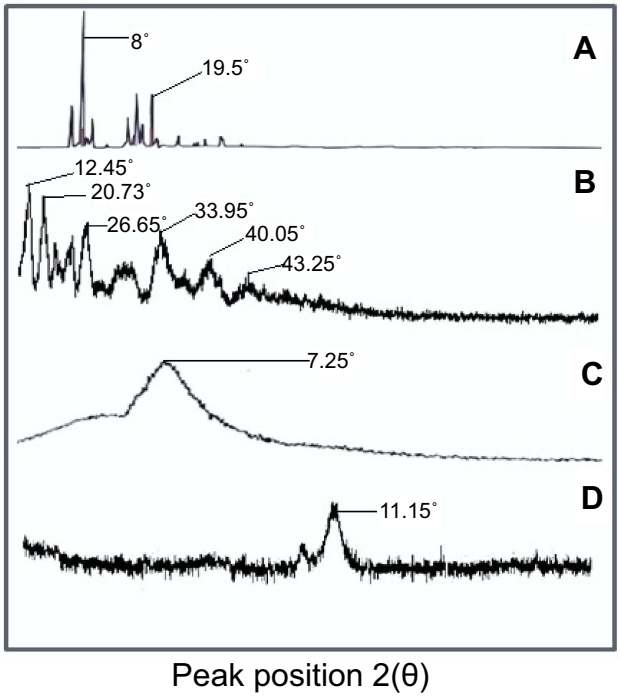

Figure 5 XRD diffractograms of lovastatin (**A**), β-cyclodextrin (**B**), montmorillonite (**C**), and nanocomposite hydrogels (**D**).
Abbreviation: XRD, X-ray diffraction.

significantly varied, confirming the better effect of the drug when incorporated into NC network.

Acute oral toxicity studies

During the whole toxicity study duration each group was intensely monitored for fluid and food intake, body weight, common disease symptoms including temperature, restlessness, diarrhea, and signs of dermal and ocular toxicity. Body weight of rabbits was recorded before the start of toxicity study, Day 1, Day 7, and Day 14. It was observed that there were no significant changes after administering NC networks. No signs of dermal and ocular toxicity were seen. Moreover, death rate was zero. To circumvent such issues hematological, biochemical, and histopathological parameters were also evaluated. Overview of these prominent parameters is tabulated in Tables 5, 6 and 7 and Figure 10.

Discussion

Sol – Gel contents of developed NC networks were determined in order to estimate sol and gel percentage within final formulations. Sol fraction includes unreactive reactants, ie, polymer, monomer, and crosslinker soluble in distilled water. Gel fraction reflects the degree of grafting and crosslinking density. When various quantities of MAA (BM1 – BM3) were incorporated there was an increase in gel fraction from 72.75%–80.18%. While in the case of MBA-containing formulations (BM-4 – BM-6) %gel fraction ranged within

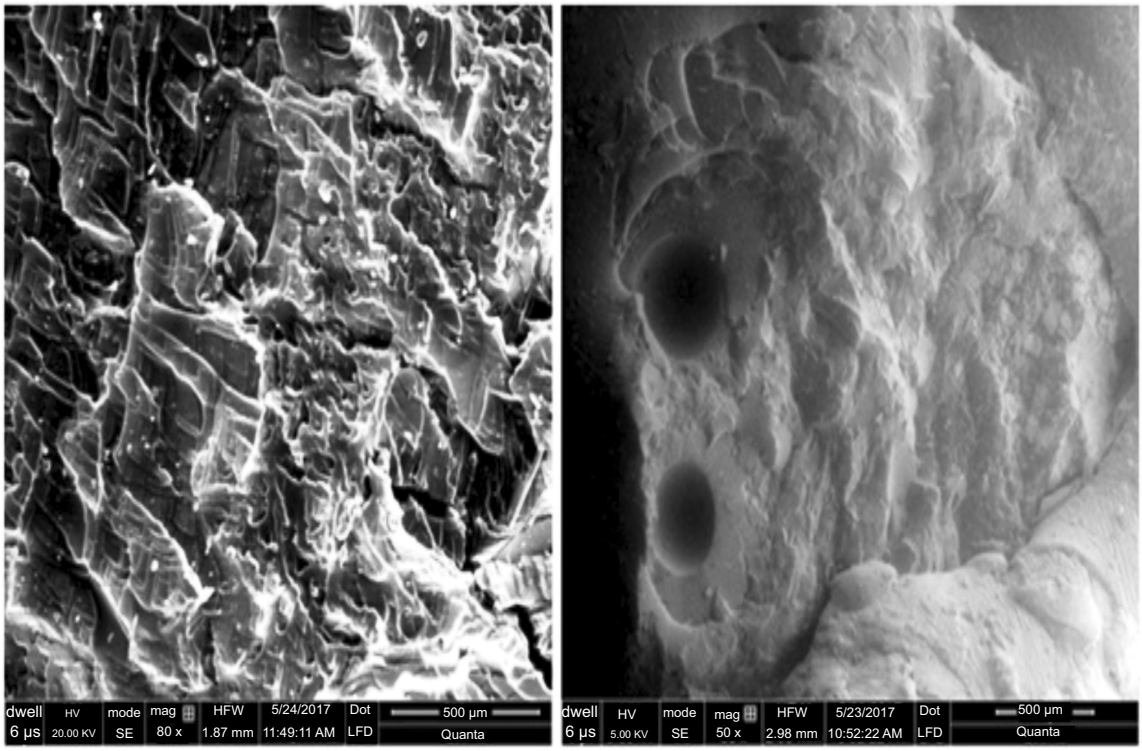

Figure 6 SEM micrographs of NC hydrogels (BM-8).
Abbreviations: SEM, scanningelectron microscopy; NC, nanocompsite.

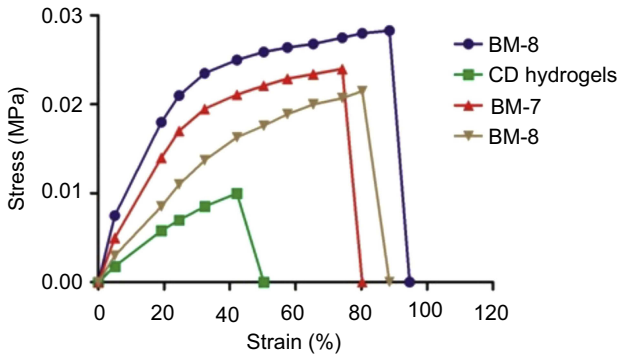

Figure 7 Tensile stress – strain curves.
Abbreviation: CD, cyclodextrin.

82.51%–91.85% due to higher crosslinking density. Optimum %gel fraction values were observed in MMT-containing formulations (BM-7 – BM9) ie, 87.15%–95.22% due to the fact that MMT has (-Si – OH) groups on its surface responsible for bonding with water soluble polymers thereby promoting crosslinking with carboxylate ($-COO^-$) ions of MAA.[26] Similar trends of %gel fraction improvement have also been reported by Sirousazer et al, 2011.

IR pattern of LVT reflected a number of evident peaks because of different structural functional groups at 3537.45 cm^{-1} (-OH stretching vibrations), 2927.94 cm^{-1}, and 1697.25 cm^{-1} (bending vibration of C=O group of lactone ring), 1219.11 cm^{-1} (stretching vibrations of C-O group of alcohol), 1261.45 cm^{-1} (bending vibrations of C-O-C group of lactone ring). IR spectrum of MAA exhibited a broad band at 2990.31 cm^{-1} due to –OH groups. A strong absorption peak at 1695.85 cm^{-1} corresponds to carboxylic acid groups.

In β-CD IR spectrum, a broad band was seen at 3321.11 cm^{-1} due to O-H stretching. Other peaks at 2735.15 cm^{-1}, 1645.25 cm^{-1}, and 1033.21 cm^{-1} corresponds to C-H stretching, H-O-H bending, and C-O-C stretching, respectively. IR spectrum of MMT showed slightly wide absorption bands at 3477.17 cm^{-1} and 3626.16 cm^{-1} due to H-O-H stretching vibrations of interlayer water and Si-O-H, respectively.[27] Broadness around 3619.17–3033.21 cm^{-1} is

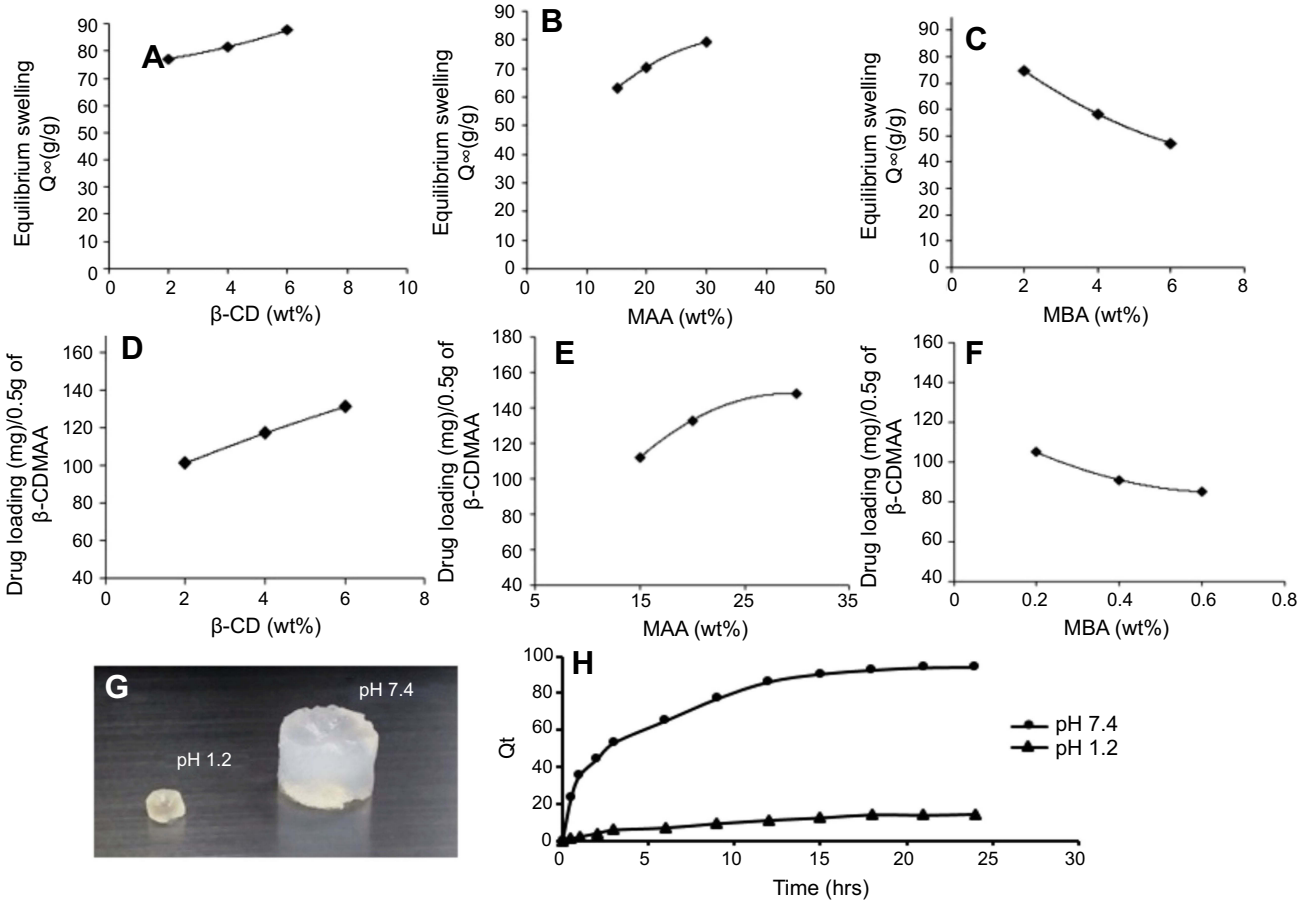

Figure 8 Effect of (**A, D**) MMT content (**B, E**) MAA content (**C, F**) MBA content on swelling and LVT loading on NC networks, (**G, H**) pH on physical and dynamic swelling.
Abbreviations: CD, cyclodextrin; MMT, montmorillonite; MAA, methacrylicacid; MBA, methylene bisacrylamide; LVT, lovastatin; NC, nanocomposite.

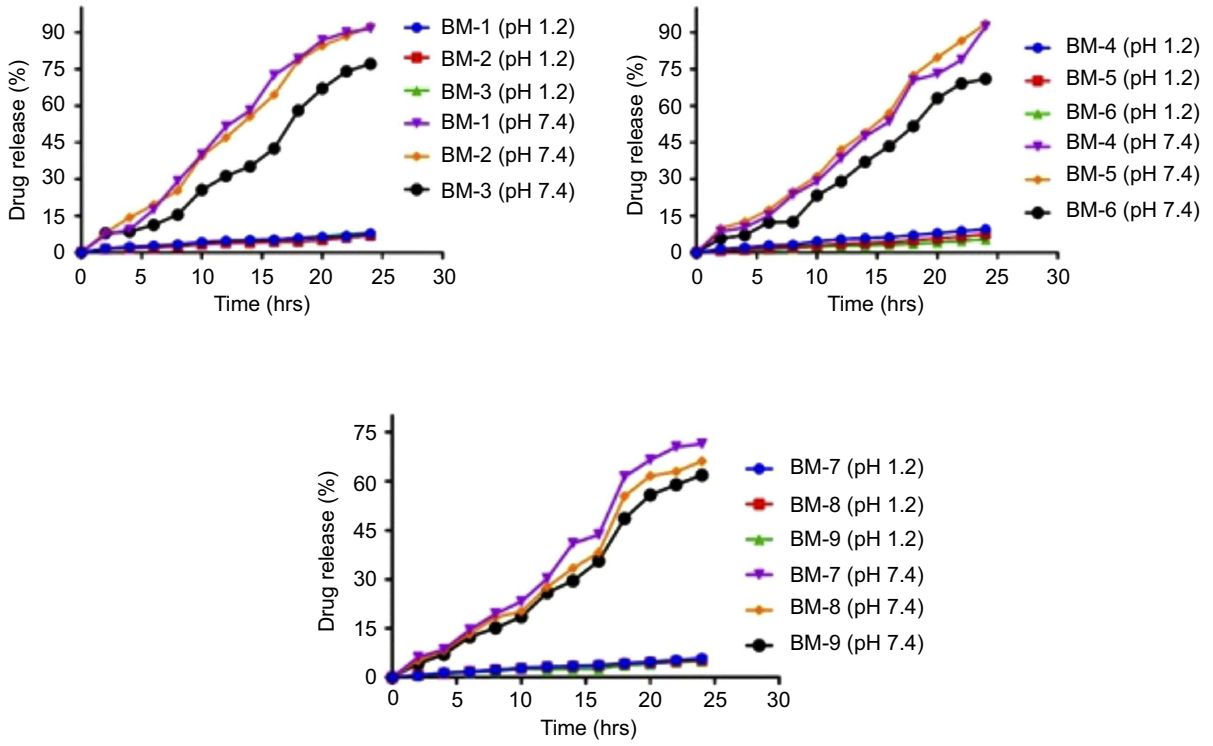

Figure 9 Lovastatin release studies at pH 1:2 and pH 7.4.

Table 2 Results of lovastatin release kinetics studies

Formulation	Zero order	First order	Higuchi	Korsemeyer Peppas	
	R^2	R^2	R^2	R^2	n
BM-1	0.9805	0.9031	0.8232	0.9813	1.046
BM-2	0.9886	0.9054	0.8271	0.9903	1.068
BM-3	0.9528	0.8702	0.7380	0.9867	1.377
BM-4	0.9773	0.8851	0.7818	0.9927	1.233
BM-5	0.9826	0.8851	0.7949	0.9938	1.193
BM-6	0.96.9	0.8838	0.7474	0.9903	1.341
BM-7	0.9672	0.8903	0.7739	0.9816	1.223
BM-8	0.9610	0.9027	0.7626	0.9798	1.263
BM-9	0.9624	0.9028	0.7759	0.9871	1.309

evident of –OH groups in MMT structure. Short absorption band at 1631.78 cm^{-1} is due to H-O-H bending patterns of adsorbed water.[28]

No significant changes occurred in IR spectrum of the physical mixture, thereby confirming the compatibility among ingredients. A slightly different spectrum was obtained with minute reduction of intensities of peaks. While in the case of IR spectrum of LVT-loaded NC networks, different peaks with shifting of LVT characteristic peak ie, 1697.25 cm^{-1} due to C=O group of lactone ring to 1515.23 cm^{-1}, thus confirming new graft synthesis.

DSC thermogram of LVT presented a sharp endothermic peak at 173.71°C corresponding to the melting point of LVT, thus proving its crystalline nature. β-CD thermogram exhibited two endothermic peaks, ie, at 105.15°C due to loss of moisture content and at 327.39°C due to its transition from solid into liquid state. MMT revealed a broad endothermic loop near 100.06°C due to the removal of adsorbed water from the surface of MMT. As MMT remains stable at elevated temperature levels, ie, above 550°C, no further peak was seen at the set scanning range. NC network showed first endothermic peak near 95.78°C, which is due to moisture loss and second broad endothermic curve was seen near 295.13°C followed by endothermic flash at 355.17°C. Stability of developed NC hydrogel networks was significantly improved ($p<0.0021$). Morphological alterations occur due to polymerization of β-CD with other ingredients that results in an entirely different structural and characteristic profile. Thus, overall thermal degradation of NC networks was less as compared to pure ingredients, except MMT, thereby improving the stability of incorporated LVT.

TGA curves of individual ingredients as well as fabricated NC networks were recorded to estimate %weight loss with sequential rise of temperature, as summarized in Figure 4. β-CD showed degradation in two steps, ie, first decomposition phase was recorded within 30°C–105°C.

Table 3 Lipid profiles before and after treatment

Parameters	[a]Average normal values	[a]Hyperlipidemic control	After 4 weeks of treatment	
			Lovastatin suspension	[a]Lovastatin loaded nanocomposite networks
Total cholesterol (mg/dL)	45.01±13.75	945.11±616.91	761±36.85	277.23±12.1
Triglycerides (mg/dL)	48.25±15.05	77.53±6.45	62±5.28	38.86±2.66
Low density lipoprotein (mg/dL)	18.23±15.33	522.24±21.88	390.11±28.1	147.63±31.5
Highdensity lipoprotein (mg/dL)	24.55±5.31	58.95±5.67	61.25±5.37	67.11±5.11

Note: [a]Average of three determinations; ± SD.

Approximately 13.28% weight loss occurred due to escape of crystal water from the pockets of β-CD. Second decomposition phase with 79.24% weight loss was recorded between 273.16°C–327.15°C (near melting temperature of β-CD). Degradation of LVT started from 171.06°C ie, above the melting point of LVT with %weight loss of 55.13% due to breakdown of lactone ring. On further increment of temperature ie, up to 400.29°C, almost 82.15% LVT was decomposed. MMT TGA curve revealed only 10% weight loss at 109.12°C. MMT has a melting temperature above 550°C, therefore no further mass reduction was observed. Moreover, stability of developed NC networks was improved as compared to individual contents, ie, LVT, β-CD, and MAA. Initial mass loss (18.11%) occurred above 200°C and almost 48.19% of developed NC networks had intercalated clay particles that offer resistance to volatile components produced as a result of heating. So these networks remained in intact form even at elevated temperature, ie, 374.12°C, thereby ensuring thermal stability of the network. Improvement in thermal behavior of nanocomposite hydrogels has also been reported in a study conducted by Paranhos et al, 2007.[29]

In XRD studies, the presence of sharp and intense peaks at 2Θ =8° and 19.5° confirmed the crystalline nature of LVT which is responsible for its poor dissolution of LVT. β-CD diffractogram showed sharp and evident peaks at 2Θ =12.45°, 20.73°, 26.62°, 33.65°, 40.05°, and 43.25°, thus proving the crystalline nature of the polymer. MMT diffractogram exhibited a wide and characteristic diffraction peak at 7.25° that pretends its non-amorphous nature. While in the case of diffractogram of NC networks, major peaks of LVT and β-CD were changed into fused curves. MMT peak at 2Θ =7.25° was shifted to 11.15°, as shown in Figure 5. This change might be due to the flat orientation of clay particles along with their interaction with the polymerized material. Overall, an amorphous nature was prevalent with modified structural and mechanical properties. Amorphous forms offer better dissolution as compared to the crystalline forms. A similar fact has been revealed in another study conducted by Daralan et al, 2009.[30]

SEM analysis revealed that NC networks' surfaces had distributed pores and cracks in their morphology. The presence of pores facilitates uptake of water or biological fluid that maximizes capillary effect and surface area. Ionic and hydrophilic groups from the NC networks and method of drying collectively resulted in surfaces having

Table 4 Statistical evaluation for comparative analysis of hyperlipidemic control, lovastatin (LVT) suspension, and lovastatin loaded nanocompsite networks

Tukey's multiple comparison test	Mean difference	R^2	Significant? $p<0.05$?	Summary
Total cholesterol				
Hyperlipidemic control vs LVT suspension	184.0	>0.99	Yes	***
Hyperlipidemic control vs LVT-loaded NC networks	668.0	>0.99	Yes	***
LVT suspension vs LVT-loaded NC networks	483.9	>0.99	Yes	***
Triglycerides				
Hyperlipidemic control vs LVT suspension	17.18	>0.98	Yes	***
Hyperlipidemic control vs LVT-loaded NC networks	38.89	>0.98	Yes	***
LVT suspension vs LVT-loaded NC networks	21.71	>0.98	Yes	***
Low density lipoprotein				
Hyperlipidemic control vs LVT suspension	132.0	>0.99	Yes	***
Hyperlipidemic control vs LVT-loaded NC networks	374.9	>0.99	Yes	***
LVT suspension vs LVT-loaded NC networks	242.8	>0.99	Yes	***
High density lipoprotein				
Hyperlipidemic control vs LVT suspension	−1.767	>0.7	No	Ns
Hyperlipidemic control vs LVT-loaded NC networks	−8.720	>0.9	Yes	*
LVT suspension vs LVT-loaded NC networks	−6.953	>0.9	Yes	*

Note: Asterisks indicate the intensity of the significance. *p*-value value less than 0.05 is significant. Values less than but closer to 0.05 are indicated by single star (*) while values far less than the 0.05 are presented by (***).

Table 5 Clinical observations during acute oral toxicity studies

Observation	Group I (control)	Group II (treated with NC networks 5 g/kg)
Symptoms of illness	Nil	Nil
Body weight (kg)		
Pretreatment	2.02±0.05	2.03±0.05
Day 1	2.04±0.03	2.04±0.04
Day 7	2.06±0.04	2.06±0.04
Day 14	2.07±0.06	2.08±0.07
Water intake (mL)		
Pretreatment	188.45±1.45	193.33±0.06
Day 1	194.55±2.05	192.45±1.92
Day 7	201.15±3.05	196.11±2.85
Day 14	207.43±2.64	201.35±2.05
Food intake (g)		
Pretreatment	71.13±1.05	72.45±1.45
Day 1	72.53±1.51	70.11±1.12
Day 7	73.23±1.67	76.43±1.75
Day 14	75.33±1.32	71.11±1.05
Dermal toxicity	Nil	Nil
Ocular toxicity	Nil	Nil
Mortality	Nil	Nil

Note: All values are expressed as mean ± SD (n=3).

Table 6 Results of biochemical analysis of rabbits' blood

Parameter	Group I (control)	Group II (treated with nanocomposite networks 5 g/kg)
Hemoglobin (g/dL)	12.55±0.55	12.68±0.51
pH	6.97±0.21	7.01±0.19
White blood cells ($\times 10^{9L-1}$)	6.77±0.07	7.15±0.25
Red blood cells ($\times 10^{6} mm^{-3}$)	6.40±0.23	6.38±0.35
Platelets ($\times 10^{9L-1}$)	4.35±0.27	4.65±0.19
Monocytes (%)	3.43±0.35	3.51±0.21
Neutrophils (%)	55.55±2.03	55.95±2.01
Lymphocytes (%)	64.95±3.85	64.71±3.75
Mean corpuscular volume (%)	65.01±2.95	64.01±3.51
Mean corpuscular hemoglobin (pg/cell)	22.7±0.70	21.93±0.73
Mean corpuscular hemoglobin concentration (%)	31.5±1.15	33.45±2.65

Note: All values are expressed as mean ± SD (n=3).

Table 7 Kidney, liver, and lipid profile of NC network-treated rabbits

Biochemical analysis	Group I (control)	Group II (treated with nanocomposite networks 5 g/kg)
ALT (IU/L)	156.23±5.53	163. 12±11.5
AST (IU/L)	61±3.55	77.21±5.75
Urea (mmol/L)	14.35±0.51	16.25±2.53
Creatinine (mg/dL)	1.15±0.13	1.15±0.24
Uric acid (mg/dL)	3.15±0.13	3.21±0.11
Cholesterol (mg/dL)	65.16±5.23	63.15±5.95
Triglycerides (mg/dL)	54.75±6.85	65.25±4.21

Note: All values are expressed as mean ± SD (n=3).

voids in them. Smooth surfaces and presence of solid mass favored the development of a stable network.

A successive rise in tensile strength was noted while switching from BM-7 to BM-8. A increase in MMT amount facilitated further crosslinking between MMT and polymer and mechanical strength too. In these two formulations, the texture of NC networks remained smooth without any sort of brittleness. However, further rise in MMT content (BM-9) resulted in aggregation with surrounding MMT particles, thereby badly affecting mechanical strength of developed NC networks.

Li et al, in 2017, developed polyurethane and polyvinyl alcohol networks with different masses of silver particles. A similar pattern in results was observed as seen in our findings.[31]

The effect of MMT, MAA, and MBA on LVT loading and swelling of NC networks was evaluated. Formulations (BM-1 – BM-3) with rising methacrylic load exhibited promotional behavior of swelling ie, from 61.15%–83.43% ($p<0.0094$) (Figure 8B). This rise in swelling can be related to the availability of a higher number of carboxylic groups (pKa = ~4.5–5). At pH 7.4, these groups are ionized to impart strong polymeric repulsion, thus generating free volume within the networks for more uptake of media. Similar potential of MAA has already been seen in other studies conducted by Seeli and Prabaharan, 2017.[32]

The effect of increasing MBA content on swelling of NC networks was also evaluated, as shown in Figure 8C. With the increasing content of MBA, swelling was decreased ie, 74.55%–49.55% ($p<0.0075$). This might be due to the fact that increasing MBA concentrations potentiate crosslinking density, retard diffusion process, reduce interconnected pores, and provide hindrance in polymeric chain mobility. Similar type of findings has been depicted in another study conducted by Olad et al, 2018.[18]

The effect of MMT on NC hydrogel swelling was also observed at variable feed rate. It was noticed that initially with the rise of MMT contents (up to 20% of polymer and monomer contents) swelling was increased from 71.45 g/g to 91.44 g/g. This enhancement of swelling ratio and expansion of NC network was due to strong electrostatic repulsions between negative charge on MMT surface and carboxylic groups govern from MAA. Swelling ratio was

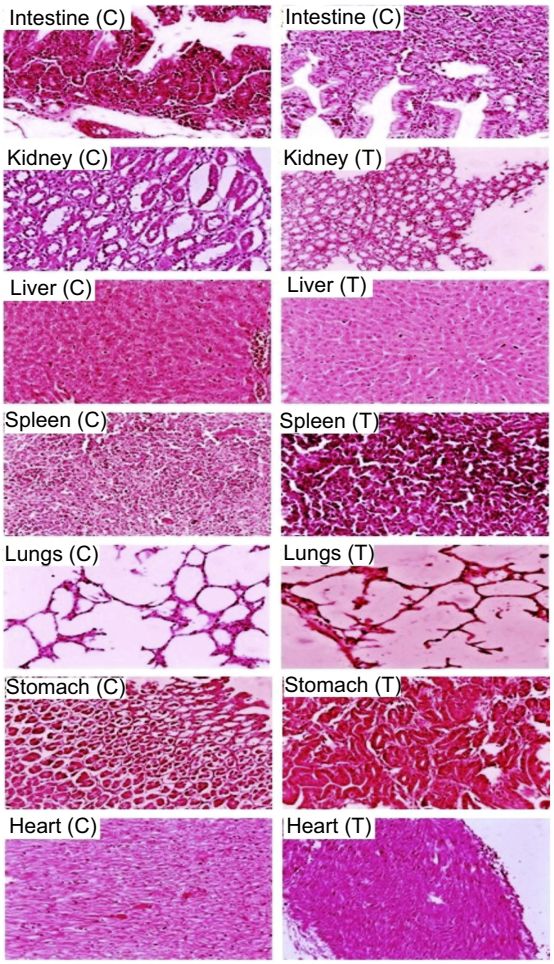

Figure 10 Histopathological examination of vital organs of rabbits after administration of β-CD-g-MAA NC networks (BM-8) (5 g/kg) in control group (C) and treated group (T).
Abbreviations: CD, cyclodextrin; MAA, methacrylicacid; NC, nanocomposite.

decreased from 91.44 g/g to 80.42 g/g on further rise of MMT contents (>20%). This was attributed to rise in physical crosslinking density. The same effect of MMT on swelling ratio has been revealed in a study conducted by Olad et al, 2018.[18]

Various amounts of LVT were loaded into the prepared NC hydrogel discs depending upon quantity, characteristic features of the ingredients, and pH of the medium, as reflected in Figure 8 (D–F). LVT loading was assisted by swelling diffusion process and pH of the medium. pH-sensitive behavior was noticed. Higher swelling was seen at pH 7.4 instead of pH 1.2, as there is more electrostatic repulsion among ionized functional groups, as shown in Figure 8(G, H).

As MAA amount was increased, LVT release experienced a continuous decrease. Maximum release, ie, 86.84% was achieved through formulation BM-4. But above a specific MAA level, LVT release was reduced to 71.44% (BM-6) at pH 7.4. This change might be due to the rise in crosslinking density, dense structure, more viscosity, poor solvent penetration, and capillary action.

Likewise, MBA rise also affected LVT release from the carrier system, as these formulations (BM-7 – BM-9) contain MMT with increasing profile too. Both of these components participate in crosslinking phenomenon. With the increasing increment of both there was a decrease in LVT release to 61.89% (BM-9) at pH 7.4. These ingredients promote crosslinking and MAA reduces LVT release, as per aforementioned reasons.

Best fit model was zero order based on R^2 values ie, 0.9528–0.9886. Thus, this carrier system has proven sustained release of LVT with acceptable variations. The mechanism of LVT release from these networks was determined from exponent "n" value. Value of "n" was greater than 0.89, indicating Super Case II transport.

In antihyperlipidemic studies, elevated lipid profile was obtained after continual administration of an atherogenic diet for 30 days. Total cholesterol content was increased to 945.11±13.75 mg/dL from 45.01±12.1 mg/dL. TG level was also raised from 48.25±15.05 mg/dL to 77.53 ±6.45 mg/dL. Moreover, LDL and HDL levels were also enhanced from 18.23±15.33 mg/dL to 522.24±21.88 mg/dL and 24.55±5.31 mg/dL to 58.95±5.67 mg/dL, respectively, as shown in Table 3.

After induction of hyperlipidemia, LVT-loaded NC networks were administered in hard gelatin shells (6 mg/kg/day) followed by 5–10 mL water for 30 days. After this treatment period, samples were again drawn in EDTA tubes to record lipid levels. A decrease in lipid levels was noticed. Total cholesterol was decreased to 277.23±12.1 mg/dL while TG and LDL levels were also decreased to 38.86±2.66 mg/dL and 147.63±31.5 mg/dL from 77.53±6.45 mg/dL and 522.24 ±21.88 mg/dL, respectively. In contrast to this, HDL level was slightly increased to 67.11±5.11 mg/dL (even higher than hyperlipidemic levels, ie, 58.95±5.67 mg/dL). Rise in HDL levels supports the hypolipidemic effect of LVT-loaded NC networks. Mehta et al, in 2003, checked hypocholesterolemic potentials of *Moringa oleifera* and LVT in hypercholesteremic rabbits. In their findings, a cholesterol-lowering effect was observed in all parameters ie, TG, LDL, and TG, except for HDL levels, as seen in our studies.[33]

Biocompatibility of reactants ie, β-CD, MAA, MMT, MBA, and APS as well as fabricated NC networks with a living system is a challenging task. Soluble unreactive species leaching out of the developed network can impart toxic effects on living tissues of any organ.

During hematological analysis, blood samples (2–3 mL) were drawn from marginal vein into EDTA tubes to void coagulation of blood taken. Plasma was separated after centrifugation of each blood sample separately (Hitachi Zentrifugen EBA 20, Hitachi Ltd., Tokyo, Japan) at 5,000 rpm for 10 minutes. Moreover, histopathological examinations of tissue sections of vital organs revealed no sign of lesion, disruption, inflammation, and abnormality under light microscope (×40). No mortality was reported in studied groups. Furthermore, no histopathological destruction was seen in vital organs. Cardiac section showed that myocytes were precisely arranged and retained their shape without any necrotic and inflammatory signs.

Liver sections of control and treated groups were also evaluated microscopically. In both groups no sign of disruption or degeneration was seen. Hepatic cord and lobules were arranged in a good manner. There was no cellular invasion of defender cells like macrophages, monocytes, neutrophils, and lymphocytes in hepatocytes.

Lung microscopic evaluation showed no indication of abnormalities in lungs. Bronchioles had a normal appearance without any sort of inflammation and cellular damage. Likewise, optical micrographs of rabbit's kidney section indicated definite renal cell structure containing nuclei. There was no indication of bleeding, hemorrhage, and cell degeneration.

Furthermore, the shape of spleen cells remained unaltered in both control as well as treated group with β-CD-g-poly (MAA) nanocomposite networks. Various researchers from Pakistan have already conducted toxicity studies to ensure safety of living systems against developed crosslinked networks ie, β-CD-g-MAA hydrogel microparticles (Mahmood et al, 2016), polyvinyl alcohol and itaconic acid–g–MAA combinatorial networks (Orva et al, 2018), cellulose acetate phthalate–g–MAA networks (Shah et al, 2018), and chondroitin sulfate–g–MAA (Barkat et al, 2018) etc.[34–36] Our results were comparable with the findings of these studies. So, the developed network was safe and biocompatible for the use of oral delivery of drugs.

Conclusion

A novel pH-responsive crosslinked network containing β-CD -g-poly (MAA) polymer and MMT was developed which swelled at basic pH (pH 7.4) to release the incorporated LVT. It has proven its usefulness by delivering LVT at higher pH region without any instability issue, even in the absence of any coating. Comparative tensile strength analysis had proven that MMT containing NC hydrogels exhibits a better mechanical profile as compared to networks of this combination. Optimized formulations with biocompatible, non-toxic, and potentially safe nature were successfully prepared for controlled delivery of drugs.

Limitations

While designing nanocomposite hydrogels, close control on physicochemical properties is required and additional studies are required to explain briefly, the interaction of therapeutic moieties either with the clay or with the polymeric chains of the developed network. Moreover, 100% drug contents are not removed from these networks.

Future prospects

The present work can be extended further by incorporating drugs requiring persistent release in long-term therapies like cancer etc. Moreover, extensive work is required to understand polymeric interactions with MMT or other nanomaterials.

Acknowledgments

The authors are deeply grateful to Higher Education Commission (HEC) of Pakistan for providing funds in the form of Start-up Research Grant Programme (reference number 21-1196/SRGP/R&D/HEC/2016) to Dr. Asif Mahmood.

Disclosure

The authors report no conflicts of interest in this work.

References

1. Al-Rashida M, Haider A, Kortz U, Joshi SA, Iqbal J. Development and in vitro anticancer evaluation of self-assembled supramolecular ph responsive hydrogels of carboxymethyl chitosan and polyoxometalate. *Chem Select*. 2018;3(5):1472–1479.
2. Su X, Chen B. Tough, resilient and pH-sensitive interpenetrating polyacrylamide/alginate/montmorillonite nanocomposite hydrogels. *Carbohy Polym*. 2018;197:497–507. doi:10.1016/j.carbpol.2018.05.082
3. Song F, Li X, Wang Q, Liao L, Zhang C. Nanocomposite hydrogels and their applications in drug delivery and tissue engineering. *J Biomed Nanotech*. 2015;11(1):40–52. doi:10.1166/jbn.2015.1962
4. Zheng JP, Li P, Ma YL, Yao KD. Gelatin/montmorillonite hybrid nanocomposite. I. Preparation and properties. *J App Polym Sci*. 2002;86:1189–1194. doi:10.1002/app.11062
5. Lee WF, Jou LL. Effect of the intercalation agent content of montmorillonite on the swelling behavior and drug release behavior of nanocomposite hydrogels. *J App Polym Sci*. 2004;94(1):74–82. doi:10.1002/app.20730
6. Karimi A, Wan Daud WM. Materials, preparation, and characterization of PVA/MMT nanocomposite hydrogels: a review. *Polym Comp*. 2017;38(6):1086–1102. doi:10.1002/pc.23671
7. Guan Q, Chen W, Hu X. Development of lovastatin-loaded poly (lactic acid) microspheres for sustained oral delivery: in vitro and ex vivo evaluation. *Drug Design Dev Ther*. 2015;9:791. doi:10.2147/DDDT.S76676
8. Zhang Y, Zhang H, Che E, et al. Development of novel mesoporous nanomatrix-supported lipid bilayers for oral sustained delivery of the water-insoluble drug, lovastatin. *Colloids Surf B Biointerfaces*. 2015;128:77–85. doi:10.1016/j.colsurfb.2015.02.021

9. Zhou J, Zhou D. Improvement of oral bioavailability of lovastatin by using nanostructured lipid carriers. *Drug Design Dev Ther*. 2015;9:5269. doi:10.2147/DDDT.S90016
10. Leone G, Consumi M, Franzi C, et al. Development of liposomal formulations to potentiate natural lovastatin inhibitory activity towards 3-hydroxy-3-methyl-glutaryl coenzyme A (HMG-CoA) reductase. *J Drug Deliv Sci Tech*. 2018;43:107–112. doi:10.1016/j.jddst.2017.09.019
11. Liu S, Luo W, Huang H. Characterization and behaviour of composite hydrogel prepared from bamboo shoot cellulose and β-cyclodextrin. *Int J Biol Macromol*. 2016;89:527–534. doi:10.1016/j.ijbiomac.2016.05.023
12. Canbolat MF, Celebioglu A, Uyar T. Drug delivery system based on cyclodextrin-naproxen inclusion complex incorporated in electrospun polycaprolactone nanofibers. *Colloids Surf B Biointerfaces*. 2014;115:15–21. doi:10.1016/j.colsurfb.2013.11.021
13. Malik NS, Ahmad M, Minhas MU. Cross-linked β-cyclodextrin and carboxymethyl cellulose hydrogels for controlled drug delivery of acyclovir. *PLoS One*. 2017;12(2):e0172727. doi:10.1371/journal.pone.0172727
14. Heydari A, Sheibani H. Fabrication of poly (β-cyclodextrin-co-citric acid)/bentonite clay nanocomposite hydrogel: thermal and absorption properties. *RSC Adv*. 2015;5(100):82438–82449. doi:10.1039/C5RA12423A
15. Meenach SA, Otu CG, Anderson KW, Hilt JZ. Controlled synergistic delivery of paclitaxel and heat from poly (β-amino ester)/iron oxide-based hydrogel nanocomposites. *Int J Pharm*. 2012;427(2):177–184. doi:10.1016/j.ijpharm.2012.01.052
16. Hua S, Yang H, Wang W, Wang A. Controlled release of ofloxacin from chitosan–montmorillonite hydrogel. *Appl Clay Sci*. 2010;50(1):112–117. doi:10.1016/j.clay.2010.07.012
17. Bounabi L, Mokhnachi NB, Haddadine N, Ouazib F, Barille R. Development of poly (2-hydroxyethyl methacrylate)/clay composites as drug delivery systems of paracetamol. *J Drug Deliv Sci Tech*. 2016;33:58–65. doi:10.1016/j.jddst.2016.03.010
18. Olad A, Zebhi H, Salari D, Mirmohseni A, Reyhanitabar A. A promising porous polymer-nanoclay hydrogel nanocomposite as water reservoir material: synthesis and kinetic study. *J Porous Mat*. 2018;1:1–11.
19. Hubert S, Chadwick A, Wacher V, Coughlin O, Kokai-Kun J, Bristol A. Development of a modified-release formulation of lovastatin targeted to intestinal methanogens implicated in irritable bowel syndrome with constipation. *J Pharm Sci*. 2018;107(2):662–671. doi:10.1016/j.xphs.2017.09.028
20. Taleb MF, Alkahtani A, Mohamed SK. Radiation synthesis and characterization of sodium alginate/chitosan/hydroxyapatite nanocomposite hydrogels: a drug delivery system for liver cancer. *Polym Bull*. 2015;72(4):725–742. doi:10.1007/s00289-015-1301-z
21. Lee DS, Hur P, Kim BK. Chemical hybridization of waterborne polyurethane with β-cyclodextrin by sol-gel reaction. *Prog Org Coat*. 2017;111:107–111. doi:10.1016/j.porgcoat.2017.04.039
22. Li JM, Hu CS, Shao JM, et al. Fabricating ternary hydrogels of P (AM-co-DMAEMA)/PVA/β-CD based on multiple physical crosslinkage. *Polymer*. 2017;119:152–159. doi:10.1016/j.polymer.2017.05.031
23. Nesrinne S, Djamel A. Synthesis, characterization and rheological behavior of pH sensitive poly (acrylamide-co-acrylic acid) hydrogels. *Arabian J Chem*. 2017;10(4):539–547. doi:10.1016/j.arabjc.2013.11.027
24. Farhadnejad H, Mortazavi SA, Erfan M, Darbasizadeh B, Motasadizadeh H, Fatahi Y. Facile preparation and characterization of pH sensitive Mt/CMC nanocomposite hydrogel beads for propranolol controlled release. *Int J Bio Mac*. 2018;111:696–705. doi:10.1016/j.ijbiomac.2018.01.061
25. Zhong M, Liu YT, Xie XM. Self-healable, super tough graphene oxide–poly (acrylic acid) nanocomposite hydrogels facilitated by dual cross-linking effects through dynamic ionic interactions. *J Mat Chem B*. 2015;3(19):4001–4008. doi:10.1039/C5TB00075K
26. Sirousazar M, Kokabi M, Hassan ZM, Bahramian AR. Dehydration kinetics of polyvinyl alcohol nanocomposite hydrogels containing Na-montmorillonite nanoclay. *Sci Iran*. 2011;18(3):780–784.
27. Jain S, Datta M. Montmorillonite-alginate microspheres as a delivery vehicle for oral extended release of venlafaxine hydrochloride. *J Drug Deliv Sci Tech*. 2016;33:149–156. doi:10.1016/j.jddst.2016.04.002
28. Ledeti IO, Vlase G, Vlase T, et al. Instrumental analysis of potential lovastatin—excipient interactions in preformulation studies. *Rev Chim (Bucharest)*. 2015;66(6):879–882.
29. Paranhos CM, Soares BG, Oliveira RN, Pessan LA. Poly (vinyl alcohol)/clay-based nanocomposite hydrogels: swelling behavior and characterization. *Macromol Mat Eng*. 2007;292(5):620–626. doi:10.1002/mame.200700004
30. Dalaran M, Emik S, Güçlü G, İyim TB, Özgümüş S. Removal of acidic dye from aqueous solutions using poly (DMAEMA–AMPS–HEMA) terpolymer/MMT nanocomposite hydrogels. *Polym Bull*. 2009;63(2):159–171. doi:10.1007/s00289-009-0077-4
31. Li X, Jiang Y, Wang F, et al. Preparation of polyurethane/polyvinyl alcohol hydrogel and its performance enhancement via compositing with silver particles. *RSC Adv*. 2017;7(73):46480–46485. doi:10.1039/C7RA08845K
32. Seeli DS, Prabaharan M. Guar gum oleate-graft-poly (methacrylic acid) hydrogel as a colon-specific controlled drug delivery carrier. *Carbohyd Polym*. 2017;158:51–57. doi:10.1016/j.carbpol.2016.11.092
33. Mehta K, Balaraman R, Amin AH, Bafna PA, Gulati OD. Effect of fruits of Moringa oleifera on the lipid profile of normal and hypercholesterolaemic rabbits. *J Enthnopharm*. 2003;86(2–3):191–195. doi:10.1016/S0378-8741(03)00075-8
34. Abdullah O, Usman Minhas M, Ahmad M, Ahmad S, Barkat K, Ahmad A. Synthesis, optimization, and evaluation of polyvinyl alcohol-based hydrogels as controlled combinatorial drug delivery system for colon cancer. *Adv Polym Tech*. 2018. doi:10.1002/adv.22119
35. Mahmood A, Ahmad M, Sarfraz RM, Minhas MU. β-CD based hydrogel microparticulate system to improve the solubility of acyclovir: optimization through in-vitro, in-vivo and toxicological evaluation. *J Drug Deliver Sci Tech*. 2016;36:75–88. doi:10.1016/j.jddst.2016.09.005
36. Shah SA, Sohail M, Minhas MU, et al. pH-responsive CAP-co-poly (methacrylic acid)-based hydrogel as an efficient platform for controlled gastrointestinal delivery: fabrication, characterization, in vitro and in vivo toxicity evaluation. *Drug Deliv Trans Res*. 2018;9:1–23.